


## STANDARD ARTICLE

# Use of 2-dimensional speckle-tracking echocardiography to assess left ventricular systolic function in dogs with systemic inflammatory response syndrome

Andrea Corda<sup>1</sup>  | Maria Luisa Pinna Parpaglia<sup>1</sup> | Giovanni Sotgiu<sup>2</sup> | Rosanna Zobba<sup>1</sup> | Pablo Gomez Ochoa<sup>3</sup> | Jorge Prieto Ramos<sup>4</sup> | Anne French<sup>4</sup>

<sup>1</sup>Department of Veterinary Medicine, Veterinary Teaching Hospital, University of Sassari, Sassari, Italy

<sup>2</sup>Department of Biomedical Sciences, University of Sassari, Sassari, Italy

<sup>3</sup>Faculty of Veterinary Medicine, University of Zaragoza, Zaragoza, Spain

<sup>4</sup>School of Veterinary Medicine, Small Animal Hospital, University of Glasgow, Glasgow, United Kingdom

## Correspondence

Maria Luisa Pinna Parpaglia, Department of Veterinary Medicine, Veterinary Teaching Hospital, University of Sassari, Via Vienna 2, 07100 Sassari, Italy.  
Email: pinnapar@uniss.it

**Background:** Early identification of systolic dysfunction in dogs with systemic inflammatory response syndrome (SIRS) potentially could improve the outcome and decrease mortality.

**Objective:** To compare 2-dimensional speckle tracking (2D-STE) with 2-dimensional (2D) and M-mode echocardiography in the evaluation of systolic function in SIRS dogs.

**Animals:** Seventeen SIRS and 17 healthy dogs.

**Methods:** Prospective observational case-control study. Each dog underwent physical examination, conventional echocardiography, 2D-STE, and C-reactive protein measurement.

**Results:** Dogs with SIRS had lower 2D-STE ejection fraction (X4D-EF;  $44 \pm 8$  versus  $53 \pm 8$ ;  $P = .003$ ), endocardial global longitudinal strain (ENDO-G-Long-St;  $-14.6 \pm 3.2$  versus  $-18.5 \pm 4.1$ ;  $P = .003$ ), and normalized left ventricular diameter in diastole ( $1.38 \pm 0.25$  versus  $1.54 \pm 0.17$ ;  $P = .04$ ) and systole ( $0.85 \pm 0.18$  versus  $0.97 \pm 0.11$ ;  $P = .03$ ) as compared to healthy dogs. Simpson method of disks (SMOD) right parasternal EF ( $55 \pm 9$  versus  $60 \pm 6$ ;  $P = .07$ ) and end systolic volume index (ESVI;  $23 \pm 10$  versus  $21 \pm 6$ ;  $P = .61$ ), SMOD left apical EF ( $59 \pm 9$  versus  $59 \pm 6$ ;  $P = .87$ ) and ESVI ( $20 \pm 8$  versus  $22 \pm 6$ ;  $P = .25$ ), fractional shortening (FS;  $34 \pm 5$  versus  $33 \pm 4$ ;  $P = .39$ ), M-mode EF ( $64 \pm 7$  versus  $62 \pm 5$ ;  $P = .35$ ), and ESVI ( $23 \pm 11$  versus  $30 \pm 9$ ;  $P = .06$ ) were not significantly different between SIRS and control group, respectively.

**Conclusion and Clinical Importance:** Speckle tracking X4D-EF and ENDO-G-Long-St are more sensitive than 2D and M-Mode FS, EF, and ESVI in detecting systolic impairment in dogs with SIRS.

## KEYWORDS

canine, cardiovascular monitoring, echocardiography, inflammation

**Abbreviations:** 2D, 2-dimensional; 2D-STE, 2-dimensional speckle-tracking echocardiography; 3D, 3-dimensional; AHS, aided heart segmentation; BP, blood pressure; bpm, beats per minute; BSA, body surface area; BW, body weight; CRP, C-reactive protein; CV, coefficient of variation; EDV, end diastolic volume; EDVI, end diastolic volume index; EF, ejection fraction; ENDO, endocardial; ENDO-G-Long-St, endocardial global longitudinal strain; ENDO-G-Long-StR, endocardial global longitudinal strain rate; EPI, epicardial; EPI-G-Long-St, epicardial global longitudinal strain; EPI-G-Long-StR, epicardial global longitudinal strain rate; ESV, end systolic volume; ESVI, end systolic volume index; FR, frame rate; FS, fractional shortening; G, global; G-Trans-St, global transversal strain; G-Trans-StR, global transversal strain rate; HR, heart rate; LA, left atrium; Long, longitudinal; LV, left ventricle; LVIDD, left ventricular internal diameter in diastole; LVIDDN, left ventricular internal diameter in diastole normalized to body weight; LVIDS, left ventricular internal diameter in systole; LVIDSN, left ventricular internal diameter in systole normalized to body weight; PCO<sub>2</sub>, partial pressure of carbon dioxide; RR, respiratory rate; SIRS, systemic inflammatory response syndrome; SMOD, Simpson method of disks; St, strain; STE, speckle-tracking echocardiography; StR, strain rate; Tran, transversal; WBC, white blood cells; X4D-EF, XStrain 4D ejection fraction.

This is an open access article under the terms of the Creative Commons Attribution-NonCommercial License, which permits use, distribution and reproduction in any medium, provided the original work is properly cited and is not used for commercial purposes.

© 2019 The Authors. *Journal of Veterinary Internal Medicine* published by Wiley Periodicals, Inc. on behalf of the American College of Veterinary Internal Medicine.

## 1 | INTRODUCTION

Systemic inflammatory response syndrome (SIRS) is a clinical syndrome of infectious or noninfectious origin. Sepsis is a systemic inflammatory response to infection.<sup>1</sup> In canine medicine, SIRS has been reported in many infectious diseases<sup>2-6</sup> and also in several non-infectious inflammatory disorders such as pancreatitis, trauma, neoplasia, and immune-mediated diseases.<sup>2,5-10</sup> When SIRS occurs, an excessive release of cytokines results in progressive endothelial dysfunction, increased microvascular permeability and activation of the coagulation system,<sup>9,11-13</sup> which can potentially lead to secondary multiple organ dysfunction syndrome and death.<sup>1</sup> Heart rate (HR), respiratory rate (RR), body temperature, and white blood cell (WBC) count are the clinical criteria used to diagnose SIRS in veterinary<sup>14</sup> and human medicine.<sup>1</sup> Myocardial dysfunction during SIRS has been demonstrated in humans,<sup>15,16</sup> in *in vitro* models<sup>17-19</sup> and also in dogs by the lithium dilution cardiac output method.<sup>20</sup> Echocardiography has been used in only a relatively small number of studies to assess cardiac function in dogs with SIRS. The most commonly used echocardiographic indices of left ventricular (LV) systolic function such as fractional shortening (FS) and ejection fraction (EF) have not proved sufficiently sensitive to detect systolic dysfunction in dogs with SIRS<sup>21</sup> or showed systolic impairment only in non-survivor dogs.<sup>22,23</sup> Two-dimensional speckle-tracking echocardiography (2D-STE) is an echocardiographic technique that allows an objective and quantitative assessment of myocardial function by analysis of the motion of speckles created by the interaction of ultrasonic beams and the myocardium during the 2-dimensional (2D) examination. Speckle-tracking echocardiography can measure segmental, regional, and global deformation parameters such as strain (St) and strain rate (StR) in longitudinal, radial, and circumferential directions. Strain is the percentage of deformation of the myocardium during the cardiac cycle; StR is defined as the velocity at which deformation occurs. Speckle-tracking echocardiography is angle independent and allows differentiation between active and passive myocardial movements. Two-dimensional STE has been used to measure LV myocardial rotation and torsion,<sup>24</sup> radial<sup>25</sup> and longitudinal<sup>26,27</sup> St and StR, for both endocardial (ENDO) and epicardial (EPI) layers<sup>28</sup> in healthy dogs and in dogs affected by cardiac diseases.<sup>29-31</sup> In all studies, the method has been shown to have good repeatability and reproducibility. Two-dimensional STE-derived long-axis and short-axis St previously have been validated in dogs with sonomicrometry as a reference standard.<sup>32</sup> To the best of our knowledge, no previous study has analyzed LV systolic function by STE in dogs with SIRS. The main objective of our study was to compare 2D-STE with conventional 2D and M-mode echocardiography in the evaluation of systolic function in dogs with SIRS.

## 2 | MATERIAL AND METHODS

The study was an observational case-control study carried out at the Veterinary Teaching Hospital of the University of Sassari, Italy. The local ethical committee approved the study protocol and all owners signed an informed consent form before enrollment. Two groups of dogs were selected: 1 with SIRS related to different diseases and 1 without any

disorders (healthy control group). Healthy dogs were selected from a population of dogs presented for routine procedures, such as surgical castration or ovariohysterectomy. At the time of admission, each dog underwent physical examination, indirect blood pressure (BP) measurement, blood collection, and echocardiographic examination. Blood pressure was measured in lateral recumbency with a high-definition oscillometric monitor (Memodiagnostic MD 15/90 Pro, S+B medVET, Germany) with the cuff placed on a limb or on the tail. Blood pressure measurement was repeated 5 times and mean values were calculated. The following BP values were considered normal: systolic  $131 \pm 20$  mm Hg, diastolic  $74 \pm 15$  mm Hg, and mean  $97 \pm 16$  mm Hg.<sup>33</sup> Complete cell blood count (CBC; Laserocyte, Idexx Laboratories, Westbrook, Maine), serum biochemistry profile (ABX Pentra 400, Horiba Medical, Japan), and C-reactive protein (CRP) (CP2572, Randox Laboratories Limited, Crumlin, County Antrim, United Kingdom) serum concentrations were analyzed. The reference range of serum CRP concentration ranged from 0 to 1.07 mg/dL, according to information provided by the manufacturer and by a previous report.<sup>34</sup> Each echocardiographic examination was performed by a single experienced operator (Andrea Corda) with a portable ultrasound unit (My Lab Alpha, Esaote, Florence, Italy) equipped with a multifrequency 1-4 MHz phased array transducer (SP2430). Dogs were positioned alternately in right and left lateral recumbency on an echocardiographic table and examined by 2D, M-mode, Doppler, and 2D-STE with simultaneous ECG. All echocardiographic images and loops were stored and analyzed off-line by the same observer (Andrea Corda).

### 2.1 | Two-dimensional and M-mode echocardiography

M-mode and 2D cine loops and images were acquired and measured as recommended by the guidelines of the American Association of Echocardiography.<sup>35</sup> The M-mode images of the LV were obtained from the right parasternal short axis view. The M-mode-derived LV end-diastolic diameter (LVIDD) and end-systolic diameter (LVIDS) were normalized to body weight (BW)<sup>36</sup> according to the following formulas: LVIDD normalized (LVIDDN) = LVIDD (cm) / (BW [kg])<sup>0.294</sup> and LVIDS normalized (LVIDSN) = LVIDS (cm) / (BW[kg])<sup>0.315</sup>. The reference ranges of the LVIDDN and LVIDSN were 1.27-1.85 and 0.71-1.26, respectively.<sup>36</sup> The M-mode-derived LVIDD and LVIDS were used to calculate LV volumes,<sup>37</sup> EF (M-mode EF), and FS. Left ventricular volumes and EF also were calculated by the monoplane Simpson method of disks (SMOD) from the right parasternal long-axis 4-chambers view (SMOD right parasternal EF) and from the left apical 4-chambers view (SMOD left apical EF) as previously described.<sup>38</sup> Simpson and M-mode-derived end diastolic volume (EDV) and end systolic volume (ESV) were indexed to body surface area (BSA) to obtain the end diastolic volume index (EDVI) and the end-systolic volume index (ESVI).<sup>38</sup> Body surface area was calculated from BW by the following formula<sup>39</sup>:  $BSA = 0.101 \times BW \text{ (kg)}^{2/3}$ . Each echocardiographic measurement was repeated 3 times, and mean values were calculated.

### 2.2 | Two-dimensional STE analysis

Two-dimensional speckle tracking analysis was performed off-line by using 2 different software packages: 2D-XStrain (Esaote) and

XStrain-4D (Esaote). At least three 2D clips, with duration of 1 cardiac cycle each, were acquired from each of the 3 following views: (1) left apical 4-chambers showing both atria and ventricles; (2) left apical 2-chambers showing left atrium (LA) and LV; and (3) left apical 3-chambers showing LA, LV, and ascending aorta. A set of clips was composed of 3 cine-loops, 1 of each apical view. For each cine-loop, an end diastolic frame, in which ENDO and EPI borders were clearly identified, was chosen and processed by 2D-XStrain, which is a dedicated border tracking software. Left ventricular ENDO and EPI borders were delineated by 13 equidistant tracking points inserted manually under the guidance of a semiautomatic tool for border segmentation (AHS Aided Heart Segmentation, Esaote). Then, 2D-XStrain software automatically divided the LV wall, of each apical view, in 6 segments and tracked them, frame-by-frame, throughout the entire cardiac cycle. The tracking quality was visually evaluated. It was considered adequate if the tracking point movements followed the ENDO and EPI borders throughout the entire cardiac cycle. When necessary, manual adjustment of the tracking points was made. Only cardiac cycles with adequate tracking quality and with no signs of arrhythmia were included. The system used provided a quality control of the temporal resolution, it did not allow elaboration of clips having a frame rate (FR) < 40 Hz, which is adequate for HR < 100 beats per minute (bpm).<sup>40</sup> In patients with HR  $\geq$  100 bpm, to ensure an adequate temporal resolution, the LV ENDO and EPI borders were optimally visualized by adjustment of image depth, sector width, number of focal points, and line density so as to have at least 22 frames acquired for each cardiac cycle. The XStrain-4D software, by combining the results of each set of clips analyzed by 2D-XStrain, generated the LV bull's eye representation

according to the standard 17-segments model<sup>35,40</sup> (Figure 1). The XStrain-4D software provided segmental, regional, and global (G) peak systolic values of longitudinal (Long) and transversal (Tran) St and StR of both ENDO and EPI borders. The radial LV deformation observed from the apical views was denoted "transversal" by the system. The G values of peak systolic St and StR were calculated as the average of the 17 segmental peak values. The XStrain-4D software, by providing temporal compensation for HR variation and spatial alignment of the 3 apical views, produced a LV 3-dimensional (3D) reconstruction (Figure 1) and calculated LV volumes and EF<sup>41</sup> (X4D-EF) by the "Beutel model" method (Tomtec, Germany).<sup>42</sup> Three sets of clips were analyzed for each patient and mean values were calculated. The following LV XStrain-4D-derived parameters were statistically analyzed: (1) ENDO-G-Long-St, (2) ENDO-G-Long-StR, (3) EPI-G-Long-St, (4) EPI-G-Long-StR, (5) G-Tran-St, (6) G-Tran-StR, and (7) X4D-EF.

To determine intra-observer 2D-STE measurement variability, 10 echocardiograms of 10 different dogs (5 from the SIRS group and 5 from the control group) were randomly selected and submitted to 3 repeated measurements by the same observer (Andrea Corda) on the same clip sets. Each clip set was measured twice in a single day and once 1 week later to assess intra-observer within-day and between-day variability, respectively.

### 2.2.1 | Inclusion criteria

Dogs that fulfilled at least 2 of the 4 SIRS criteria<sup>14</sup> were included in the SIRS group: (1) Hypo- or hyper-thermia ( $\leq 37.8^\circ\text{C}$  or  $\geq 39.7^\circ\text{C}$ ), (2) tachycardia (HR  $\geq 160$  bpm), (3) tachypnea (RR  $\geq 40$  breaths/min) or PCO<sub>2</sub>  $\leq 32$  mm Hg, and (4) leukocytosis (WBC count  $\geq 12\,000$  WBCs/ $\mu\text{L}$ ) or leukopenia (WBC count  $\leq 4000$  WBCs/ $\mu\text{L}$ ) or  $>10\%$  band neutrophils.<sup>14</sup>

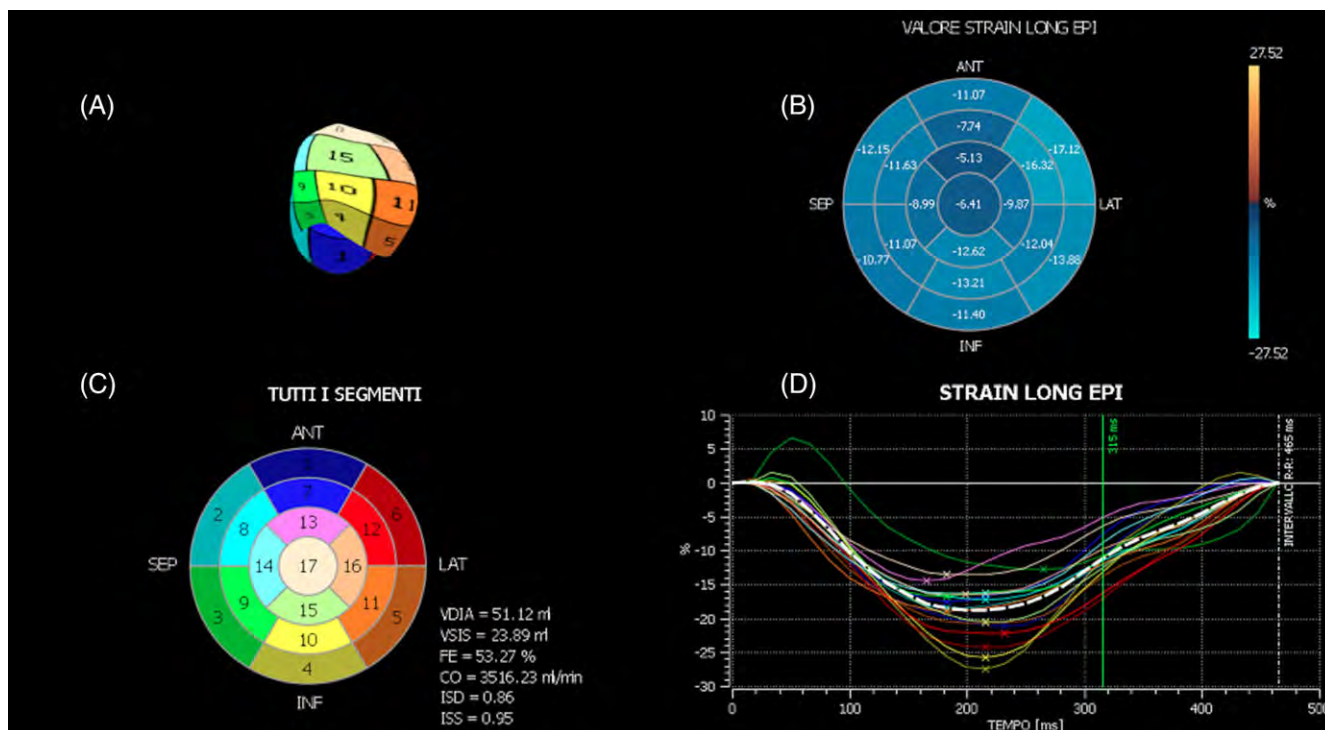


**FIGURE 1** XStrain-4D main window, after spatial alignment of the 3 apical views. A, Left ventricular 3-dimensional reconstruction; B, dynamic color coded bull's eye representation of the segmental epicardial longitudinal strain value; C, left ventricular static bull's eye representation according to the standard 17-segments model; and D, trend over time of all the segmental epicardial longitudinal strain values (colored continuous lines) and of the global epicardial longitudinal strain value (dotted white line)

Systemic inflammatory response syndrome severity was classified based on the number of SIRS criteria present at first examination.<sup>14</sup> It was defined as mild, moderate, or severe if dogs presented with 2, 3, or 4 abnormal parameters, respectively. The control group included healthy dogs based on physical examination, CBC, serum biochemical profile, BP measurement, echocardiographic examination, and serum CRP concentrations within the normal limits.

### 2.2.2 | Exclusion criteria

From the SIRS group, we excluded dogs with CRP <1.07 mg/dL,<sup>34</sup> those with thoracic trauma, and those with a previous diagnosis of hypothyroidism. From both groups, we excluded breeds of dogs most prone to dilated cardiomyopathy (Great Dane, Saint Bernard, Irish Wolfhound, Newfoundland, Doberman Pinscher, Neapolitan Mastiff, and Cocker Spaniel),<sup>43,44</sup> dogs with a previous diagnosis of cardiac disease, dogs <1 year of age, pregnant females, dogs treated with anti-inflammatory, anesthetic, sedative, or opioid drugs during the previous 12 hours, and dogs previously treated with known cardiotoxic drugs (eg, doxorubicin). From both groups, we also excluded dogs with echocardiographic evidence of congenital cardiac disease, moderate to severe valvular regurgitation (regurgitant jet area/left atrium area  $\geq 30\%$ )<sup>45</sup> with or without cardiac remodeling. Dogs with persistent arrhythmia and with Doppler echocardiography-derived evidence of pulmonary hypertension, defined as the presence of a tricuspid or pulmonic valve regurgitant jet velocity  $\geq 2.8$  or  $\geq 2.2$  m/s, respectively,<sup>46</sup> also were excluded.

### 2.2.3 | Statistical methods

Statistical analyses were performed using Stata 13 (Stata Corp, College Station, Texas). Continuous variables were presented as mean and SD or as median and interquartile ranges, depending on their parametric distribution. Student's *t* and Mann-Whitney tests were used to assess differences between control and SIRS groups. Proportion test was used to compare categorical variables. Multiple linear regression analysis was performed to explore the relationship between the 2D-STE parameters, as individual dependent variables, and dog breed, age, BW, and HR as independent variables. Statistical significance was considered when  $P < .05$ . The average percent coefficient of variation (CV) was used to quantify the within-day and between-day intra-observer measurement variability. Percent CV was calculated using the following formula:  $CV = (SD \text{ of repeated measurements} / \text{average of measurements}) \times 100$ .<sup>47</sup> The degree of variability was arbitrarily defined as follows: CV < 5%, very low variability; 5%-15%, low variability; 15%-25%, moderate variability; and >25%, high variability.<sup>48</sup> Values with CV < 15% were considered clinically acceptable.

## 3 | RESULTS

Forty dogs initially were enrolled (22 in the SIRS and 18 in the control group, respectively). Five SIRS dogs were excluded because their CRP concentrations were <1.07 mg/dL. One dog in the control group was excluded because of leukocytosis and serum CRP concentration higher than the upper normal limit. A total of 34 dogs were recruited. The SIRS group included 13 females (4 spayed) and 4 males (2 neutered), with a mean (SD) age of 7 (3.5) years and mean (SD) weight of 22.94

(11.49) kg, 8 crossbreed, 2 German Shepherd, 2 Fomni's dog, 1 Labrador Retriever, 1 English Setter, 1 Shih Tzu, 1 Epagneul Breton, and 1 Staffordshire Bull Terrier. The causes of SIRS were pyometra ( $n = 5$ ), ehrlichiosis ( $n = 3$ ), enteritis ( $n = 1$ ), pancreatitis ( $n = 1$ ), endometritis ( $n = 1$ ), leishmaniasis ( $n = 1$ ), ulcerated and metastatic mammary carcinoma ( $n = 1$ ), metastatic mast cell tumor ( $n = 1$ ), splenic and hepatic hemangiosarcoma ( $n = 1$ ), systemic lupus erythematosus ( $n = 1$ ), and secondary immune-mediated thrombocytopenia ( $n = 1$ ). Owner-reported clinical signs were anorexia ( $n = 9$ ), inappetence ( $n = 7$ ), lethargy ( $n = 7$ ), weakness ( $n = 5$ ), abdominal pain ( $n = 5$ ), polyuria and polydipsia ( $n = 3$ ), generalized pain ( $n = 2$ ), weight loss ( $n = 2$ ), vulvar discharge ( $n = 2$ ), vomiting ( $n = 2$ ), acute diarrhea ( $n = 1$ ), petechiae ( $n = 1$ ), and lameness ( $n = 1$ ). Among the SIRS dogs, 10 (59%) presented with 2 of the 4 SIRS criteria and 7 (41%) showed 3 of the 4 SIRS abnormal parameters, and were classified as having mild and moderate SIRS, respectively. No dog presented with clinical signs of severe shock such as bradycardia, hypothermia, hypotension, stupor, or coma. Median (range) duration of clinical signs before admission was 5.7 (1-30) days. All SIRS dogs underwent medical or surgical treatment or both, improved during their hospital stay, and survived until discharge. The control group included 7 females (3 spayed) and 10 males (4 neutered), with a mean (SD) age of 5.2 (2.47) years and mean (SD) BW of 19.12 (11.68) kg. They consisted of 7 crossbreeds, 3 Labrador Retrievers, 3 English Setters, 2 Staffordshire Bull Terriers, 1 Dachshund, and 1 Beagle. All 34 dogs had normal BP results. None of the 34 patients had received anti-inflammatory medications during the previous 2 weeks. Two SIRS dogs were on antibiotic treatment at the time of presentation. Four SIRS dogs showed occasional isolated ventricular premature complexes during the echocardiographic examination.

Age, BW, and sex were not significantly different ( $P > .05$ ) between SIRS and control group (Table 1). Mean serum CRP and HR were significantly higher ( $P < .05$ ) in the SIRS group (Table 1). Dogs with SIRS had mean LVIDDN and LVIDSN significantly lower ( $P < .05$ ) than healthy dogs; 4 SIRS dogs had LVIDDN and LVIDSN below the reference limits<sup>36</sup> (Table 2). All 34 dogs had M-mode-EF and FS results within normal limits, and mean values were not significantly different between groups ( $P > .05$ ; Table 2). The M-mode-derived EDVI and ESVI mean values were not significantly different between the 2 groups ( $P > .05$ ; Table 2). Mean values of the SMOD right parasternal EF and SMOD left apical EF were not significantly different between the 2 groups ( $P > .05$ ); no dog had a SMOD left apical EF < 40%, whereas only 1 dog from SIRS group had a SMOD right parasternal EF < 40% (Table 3). The SMOD right parasternal EDVI and ESVI, SMOD left apical EDVI and ESVI were not significantly different between the 2 groups ( $P > .05$ ; Table 3).

**TABLE 1** Differences in body weight (BW), age, sex, heart rate (HR) and C-reactive protein (CRP) between healthy and systemic inflammatory response syndrome (SIRS) dogs

Variable	Control (n = 17)	SIRS (n = 17)	P value
Age (months) mean (SD)	62.5 (28.9)	85.1 (42.8)	.08
BW (kg) mean (SD)	19 (12)	23 (11)	.34
Sex (male), n (%)	10 (59)	4 (24)	.08
HR (bpm) mean (SD)	106 (19)	128 (34)	.02
CRP (mg/dL) median (range)	0.14 (0-0.41)	9.64 (2.98-37.26)	.00



**TABLE 2** Differences in M-mode derived variables between systemic inflammatory response syndrome (SIRS) and control group

Variable	Control (n = 17)	SIRS (n = 17)	P value
<b>LVIDDN</b>			
Mean (SD)	1.54 (0.17)	1.38 (0.25)	.04
N dogs with LVIDDN <1.27 (%)	0	4	
<b>LVIDSN</b>			
Mean (SD)	0.97 (0.11)	0.85 (0.18)	.03
N dogs with LVIDS <0.71 (%)	0	4	
<b>FS (%)</b>			
Mean (SD)	33 (4)	34 (5)	.39
N dogs with FS <25 (%)	0 (0)	0 (0)	
<b>M-mode EDVI</b>			
Mean (SD)	79 (21)	63 (24)	.051
<b>M-mode ESVI</b>			
Mean (SD)	30 (9)	23 (11)	.06
<b>M-mode EF (%)</b>			
Mean (SD)	62 (5)	64 (7)	.35
N dogs with EF <40 (%)	0 (0)	0 (0)	

Abbreviations: EDVI, end diastolic volume index; ESVI, end systolic volume index; EF, ejection fraction; FS, fractional shortening; LVIDDN, left ventricular internal diameter at end diastole normalized to body weight; LVIDSN, left ventricular internal diameter at end systole normalized to body weight.

Speckle-tracking echocardiography resulted in technically adequate images in all dogs. Average CV for intra-observer within-day 2D-STE measurements variability ranged from 3.4% for X4D-EF to 7.6% for EPI-G-Long-St (Table 4). Average CV for intra-observer between-day 2D-STE measurements variability ranged from 4.1% for X4D-EF to 8.3% for G-Tran-St (Table 4).

Among the STE parameters analyzed, LV ENDO-G-Long-St and X4D-EF were significantly lower ( $P < .05$ ) in the SIRS dogs (Table 5). On the contrary, LV ENDO-G-Long-StR, EPI-G-Long-St, EPI-G-Long-StR, G-Tran-St, and G-Tran-StR did not show significant differences ( $P > .05$ ) between the 2 groups.

The multiple linear regression analysis results did not identify significant effects ( $P > .05$ ) of dog breed, age, and sex on X4D-EF, ENDO-G-Long-St, ENDO-G-Long-StR, EPI-G-Long-St, EPI-G-Long-StR, G-Tran-St, and G-Tran-StR (Table 6). Body weight did not have a significant effect on the 2D-STE indices of systolic function evaluated in our study, except for G-Tran-St, which was directly related to it (Table 6). Heart rate did not significantly influence the 2D-STE indices of systolic function except for EPI-G-Long-StR and G-Tran-St, which were inversely related to it.

## 4 | DISCUSSION

In our study, 2D-STE was compared with 2D and M-mode echocardiography for the assessment of LV systolic function in dogs with SIRS. Our results indicated that mild to moderate stages of SIRS in dogs were associated with LV systolic impairment identified by 2D-STE ENDO-G-Long-St and X4D-EF, but not detected by 2D- and M-mode-derived EF, FS, and ESVI.

The 2D-STE software we used in our study (XStrain-4D) enabled assessment of layer-specific longitudinal deformation as

**TABLE 3** Differences in Simpson method of disks-derived variables between systemic inflammatory response syndrome (SIRS) and control group

Variable	Control (n = 17)	SIRS (n = 17)	P value
<b>SMOD right parasternal EDVI</b>			
Mean (SD)	53 (12)	49 (17)	.49
<b>SMOD right parasternal ESVI</b>			
Mean (SD)	21 (6)	23 (10)	.61
<b>SMOD right parasternal EF (%)</b>			
Mean (SD)	60 (6)	55 (9)	.07
N dogs with EF <40 (%)	0 (0)	1 (6)	
<b>SMOD left apical EDVI</b>			
Mean (SD)	55 (13)	49 (18)	.23
<b>SMOD left apical ESVI</b>			
Mean (SD)	22 (6)	20 (8)	.25
<b>SMOD left apical EF (%)</b>			
Mean (SD)	59 (6)	59 (9)	.87
N dogs with EF <40 (%)	0 (0)	0 (0)	

Abbreviations: EDVI, end diastolic volume index; EF, ejection fraction; ESVI, end systolic volume index; SMOD, Simpson method of disks.

well as transversal St and StR from the apical views. Within the myocardial wall, sub-endocardial and sub-epicardial fibers mainly are longitudinally oriented, whereas the mid-wall fibers are circumferentially oriented.<sup>49</sup> Results from our investigation suggested that mild and moderate stages of SIRS in dogs affected LV longitudinal endomyocardial shortening without altering either longitudinal epimyocardial or radial contraction. A potential explanation could be that ischemia, induced by SIRS-associated microcirculatory alterations,<sup>12,50</sup> coupled with possible higher sensitivity of the sub-endocardial myocytes to the direct negative effect of the inflammatory mediators, could affect firstly, and more severely, the longitudinally oriented sub-endocardial myocytes rather than the circumferential mid-wall and longitudinal sub-epicardial fibers, leading to a decrease in endomyocardial longitudinal systolic shortening. The sub-endocardial myocytes are the first fibers affected by imbalance in oxygen delivery and coronary blood supply<sup>51,52</sup> because of the fact that O<sub>2</sub> consumption, ATP utilization, and fiber contraction are higher in the sub-endocardial layer than in

**TABLE 4** Between-day and within-day intra-observer 2-dimensional speckle-tracking echocardiography (2D-STE) measurements variability

Variable	Average intra-operator CV (%)	
	Between-day (n = 10)	Within-day (n = 10)
X4D-EF (%)	4.1	3.4
ENDO-G-Long-St	6.3	5.4
ENDO-G-Long-StR	4.8	5.2
EPI-G-Long-St	5.2	7.6
EPI-G-Long-StR	5.2	6.7
G-Tran-St	8.3	6.7
G-Tran-StR	8.1	7.2

Abbreviations: CV, coefficient of variation; ENDO-G-Long-St, endocardial global longitudinal strain; ENDO-G-Long-StR, endocardial global longitudinal strain rate; EPI-G-Long-St, epicardial global longitudinal strain; EPI-G-Long-StR, epicardial global longitudinal strain rate; G-Tran-St, global transversal strain; G-Tran-StR, global transversal strain rate; X4D-EF, XStrain-4D-derived ejection fraction.

**TABLE 5** Differences in 2-dimensional speckle tracking-derived variables between systemic inflammatory response syndrome (SIRS) and control group

Variable	Control (n = 17)	SIRS (n = 17)	P value
<b>X4D-EF (%)</b>			
Mean (SD)	53 (8)	44 (8)	.00
<b>ENDO-G-Long-St (%)</b>			
Mean (SD)	-18.5 (4.1)	-14.6 (3.2)	.00
<b>ENDO-G-Long-StR (1/s)</b>			
Mean (SD)	-1.9 (0.3)	-1.7 (0.4)	.17
<b>EPI-G-Long-St (%)</b>			
Mean (SD)	-16.2 (3)	-15 (4.1)	.34
<b>EPI-G-Long-StR, (1/s)</b>			
Mean (SD)	-1.6 (0.3)	-1.7 (0.5)	.69
<b>G-Tran-St (%)</b>			
Median (range)	25.6 (12.6-41.6)	21.2 (8.1-31.9)	.27
<b>G-Tran-StR (1/s)</b>			
Mean (SD)	2.8 (0.6)	2.5 (0.4)	.18

Abbreviations: ENDO-G-Long-St, endocardial global longitudinal strain; ENDO-G-Long-StR, endocardial global longitudinal strain rate; EPI-G-Long-St, epicardial global longitudinal strain; EPI-G-Long-StR, epicardial global longitudinal strain rate; G-Tran-St, global transversal strain; G-Tran-StR, global transversal strain rate; X4D-EF, XStrain-4D-derived ejection fraction.

the more superficial mid-wall and sub-epicardial sarcomeres.<sup>53,54</sup> An alternative explanation for failure to detect a decrease in EPI-G-Long-St in SIRS dogs, could be the fact that longitudinal EPI deformation parameters are more subject to artifacts generated by echo dropout and respiratory movements of the thorax.<sup>28</sup>

Our results indicated that the M-mode-derived LVIDDN and LVIDSN were significantly lower in the SIRS group. The decrease in LV internal diameter is an indicator of volume contraction<sup>55,56</sup> which, in the SIRS group, could be a result of dehydration secondary to anorexia or increased fluid loss by the urinary and gastrointestinal routes. Because fluid deficits have the potential to confound the echocardiographic evaluation of myocardial function,<sup>56,57</sup> we cannot eliminate the effect of decreased preload on LV ENDO-G-Long-St in our SIRS dogs, even if, among the 2D-STE parameters of deformation, global longitudinal St is considered to be less affected by load conditions.<sup>29,57</sup> Nevertheless, we speculated that decreased preload in our SIRS dogs was not relevant because G-Tran-St and EDVI, which are recognized to be highly influenced by decreased preload,<sup>29,56,58</sup> were not significantly different between the 2 groups.

Systolic impairment in SIRS dogs also was detected by 2D-STE-derived EF (X4D-EF) which was significantly decreased compared to healthy dogs. The XStrain-4D-derived EF has been validated using magnetic resonance imaging in humans,<sup>41</sup> but not in dogs. Therefore, X4D-EF reference ranges have not been established in this species. We assumed that the X4D-EF, being free of geometrical assumptions, would be more sensitive than M-mode and SMOD-derived EF in detecting systolic impairment in dogs suffering from mild to moderate SIRS. In our study, conventional 2D and M-mode indices of systolic function (FS, M-mode EF, SMOD right parasternal EF, and SMOD left apical EF) did not detect systolic dysfunction in SIRS dogs, except in 1 case in which SMOD right parasternal EF was <40%. Our results agree with those of a previous study<sup>21</sup> that did not identify echocardiographic

**TABLE 6** Effect of dog breed, age, sex, body weight (BW), and heart rate (HR) 2-dimensional speckle tracking variables

X4D-EF (%)	Beta (95% CI)	P value
Breed	0.8 (-6.75, 8.36)	.83
Age (months)	-0.01 (-0.11, 0.08)	.80
Sex (male)	2.93 (-4.06, 9.91)	.40
BW (kg)	0.15 (-0.17, 0.47)	.34
HR (bpm)	-0.1 (-0.22, 0.02)	.11
<b>ENDO-G-Long-St (%)</b>		
Breed	-0.63 (-3.79, 2.53)	.69
Age (months)	0.02 (-0.02, 0.06)	.26
Sex (male)	-0.96 (-3.87, 1.96)	.51
BW (kg)	-0.03 (-0.17, 0.1)	.63
HR (bpm)	0.05 (-0.003, 0.10)	.06
<b>ENDO-G-Long-StR (1/s)</b>		
Breed	-0.05 (-0.37, 0.27)	.76
Age (months)	0.002 (-0.002, 0.01)	.39
Sex (male)	-0.06 (-0.36, 0.24)	.70
BW (kg)	0.002 (-0.01, 0.02)	.74
HR (bpm)	-0.003 (-0.01, 0.003)	.31
<b>EPI-G-Long-St (%)</b>		
Breed	1.01 (-2.06, 4.08)	.51
Age (months)	0.01 (-0.03, 0.05)	.49
Sex (male)	-0.4 (-3.24, 2.44)	.77
BW (kg)	-0.03 (-0.16, 0.1)	.59
HR (bpm)	0.02 (-0.03, 0.07)	.34
<b>EPI-G-Long-StR (1/s)</b>		
Breed	0.05 (-0.26, 0.35)	.75
Age (months)	0.002 (-0.002, 0.01)	.38
Sex (male)	-0.01 (-0.29, 0.27)	.96
BW (kg)	0.01 (-0.01, 0.02)	.36
HR (bpm)	-0.01 (-0.01, -0.0008)	.02
<b>G-Tran-StR (1/s)</b>		
Breed	0.38 (-0.02, 0.78)	.06
Age (months)	-0.001 (-0.01, 0.004)	.70
Sex (male)	0.32 (-0.06, 0.69)	.09
BW (kg)	0.01 (-0.01, 0.02)	.43
HR (bpm)	0.003 (-0.003, 0.01)	.33
<b>G-Tran-St (%)</b>		
Breed	3.37 (-2.37, 9.11)	.24
Age (months)	-0.02 (-0.09, 0.05)	.56
Sex (male)	0.97 (-4.34, 6.28)	.71
BW (kg)	0.39 (0.14, 0.63)	.00
HR (bpm)	-0.10 (-0.19, -0.004)	.04

Abbreviations: 95% CI, 95% confidence interval of beta; Beta, coefficient of regression; ENDO-G-Long-St, endocardial global longitudinal strain; ENDO-G-Long-StR, endocardial global longitudinal strain rate; EPI-G-Long-St, epicardial global longitudinal strain; EPI-G-Long-StR, epicardial global longitudinal strain rate; G-Tran-St, global transversal strain; G-Tran-StR, global transversal strain rate; X4D-EF, XStrain-4D-derived ejection fraction.

evidence of cardiac dysfunction in a population of dogs with SIRS, based on measurements of FS and EF. On the contrary, 2 previous studies found decreases in EF and FS in dogs suffering from SIRS secondary to parvoviral enteritis,<sup>23</sup> sepsis, autoimmune diseases, and cancer.<sup>22</sup> In the first study, FS and EF were significantly decreased only in non-surviving

dogs affected by parvoviral enteritis compared with surviving and healthy dogs.<sup>23</sup> In the second study, 75% of ill dogs with FS < 26% died or were euthanized within 15 days of admission to the hospital. The reason our results differed could be a consequence of lesser severity of underlying disease in our SIRS dogs. In fact, in our study, all of the dogs improved during the hospital stay and survived until discharge. Based on these considerations, we assumed that decreased FS and EF in dogs with SIRS represent a late stage of systolic impairment which occurs after the myocardium has expended its substantial functional reserve. Two-dimensional and M-mode-derived FS and EF have some technical limitations that prevent them from detecting mild decreases in systolic function. Fractional shortening only measures LV radial contraction, without considering longitudinal and torsional deformation. The M-mode EF is inaccurate because it relies on geometric assumptions that do not apply in several cardiac diseases,<sup>35</sup> and SMOD-derived EF has poor sensitivity in detecting subclinical LV dysfunction in humans<sup>59,60</sup> and dogs.<sup>61</sup>

End systolic volume index is considered a valuable index of systolic function in dogs.<sup>62</sup> To the best of our knowledge, no study has evaluated ESVI in SIRS dogs. In our study, the ESVI values derived from M-mode, SMOD left apical 4Ch, and SMOD right parasternal 4Ch were not significantly different between the 2 groups, probably because SIRS dogs had mild systolic dysfunction that was not detectable by ESVI measurement.

Unexpectedly, none of the 2D-STE-derived StR parameters (ENDO-G-Long-StR, EPI-G-Long-StR, and G-Tran-StR) were significantly different between SIRS and healthy dogs. Because StR is a timing measurement, a possible reason for this result might be the technology itself because 2D-STE might not reach the temporal resolution needed to resolve all relevant events at a proper grade of precision, particularly in SIRS dogs, which had significantly higher HR than did healthy dogs.

Results of the comparative analysis between the SIRS and healthy dogs showed that age, BW, and sex were not significantly different, whereas, as expected, HR was significantly higher in dogs with SIRS. The effect of dog breed, age, sex, BW, and HR on 2D-STE deformation parameters was not significant in the majority of cases except for HR on G-Tran-St and EPI-G-Long-StR and for BW on G-Tran-St and G-Tran-StR. Heart rate is known to be an important modulator of cardiac function that influences several echocardiographic variables.<sup>63,64</sup> The effect of HR on 2D-STE indices of systolic function previously has been evaluated in healthy anesthetized dogs.<sup>65</sup> Results of that study showed that 2D-STE longitudinal and radial St and StR were not changed with increasing HR. On the contrary, in our study, HR was inversely related with G-Tran-St and with EPI-G-Long-StR. In agreement with our results, the decrease in 2D-STE radial St, related to an increase in HR, previously was found in a porcine model.<sup>66</sup> The shortened time of ventricular filling and the consequent decrease in venous return, secondary to increased HR, could explain this result. The effect of HR on layer-specific EPI and ENDO G-Long-StR previously has been evaluated in healthy dogs,<sup>28</sup> a study that did not find a significant effect of HR on longitudinal StR parameters. On the contrary, we found a significant inverse effect of HR on EPI-G-Long-StR. The inverse relationship between HR and the negative value of EPI-G-Long-StR means that when HR increases the absolute value of EPI-G-Long-StR increases. This result should be interpreted cautiously,

first, because the epicardial deformation could be subject to motion artifacts<sup>28</sup> and second because EPI-G-Long-StR, being a timing measurement, could be strongly conditioned by temporal resolution.

The regression analysis we performed also identified a significant direct effect of BW on G-Tran-St and StR. On the contrary, other reports did not report significant correlation between BW and radial St and StR<sup>25</sup> or found a negative correlation between radial function and BW.<sup>67</sup> These differences could be because of small sample size and the non-equal distribution of BW among the animals included in our study. Our population of dogs was not adequate for determining whether BW affected myocardial deformation, and the assessment of this effect was beyond the scope of our study.

Intra-observer within-day and between-day variability of the 2D-STE-derived indices of systolic function were considered clinically acceptable, and CV ranged from 3.4% to 8.3%. We were unable to find previously reported variability data for XStrain-4D in dogs, but our data suggest that these echocardiographic measurements are repeatable when performed by a single experienced operator.

Our study had several limitations, the most important being small sample size, which may have affected statistical power and limited inferences. Because of the small number of patients in disease categories, we did not perform further statistical analysis regarding the effect of disease category on STE variables. Another important limitation of our study was the lack of serial 2D-STE examinations in the SIRS group, which would be useful to assess LV systolic function after clinical improvement and restored loading conditions. Indeed, decreased preload, although considered not relevant in our SIRS group, could have had an effect on STE variables.<sup>29</sup> Furthermore, we did not investigate the effect of duration of clinical signs before admission, which could influence myocardial function. Another important limitation was the lack of evaluation of radial and circumferential St and StR from short-axis images, which could have added important information about systolic function during SIRS. Moreover, the STE software used in our study (XStrain-4D) has not been validated in dogs and, as a consequence, no reference ranges have been established in this species. Again, the X4D-EF was not obtained by real-time 3D speckle-tracking software, but was derived from the LV 3D reconstruction obtained by fusing together three 2D left apical views acquired in different cardiac cycles. As a consequence, although the software provided temporal compensation for the HR variation, it could be subject to errors caused by HR variability. The 2D-STE technology itself has several limitations. The accuracy of measurements is dependent on the quality of the 2D video clips being analyzed to accurately track the ENDO and EPI borders. The accuracy of STE also is dependent on the temporal resolution. Low FR results in unstable speckle patterns, whereas high FR decreases image resolution. Finally, there still are many technical differences among vendors, particularly on post-processing algorithms.<sup>35</sup>

Our study showed that some 2D-STE indices of systolic function such as ENDO-G-Long-St and X4D-EF can detect systolic impairment not identified by conventional echocardiography in dogs with mild to moderate SIRS. The early identification and treatment of systolic dysfunction in dogs with SIRS potentially could improve outcome and decrease the mortality rate.<sup>68,69</sup> Therefore, it is important to promote the use of noninvasive methods to assess cardiac function in SIRS patients. Based on our results, we believe that 2D-STE may play a pivotal role in

assessing myocardial function in dogs with SIRS. However, additional studies are needed to support more extensive use of STE to assist in the diagnosis and management of SIRS-related myocardial dysfunction.

## ACKNOWLEDGMENT

Some of these results were presented as short communication at the 27th ECVIM Congress in Malta, September 2017. We thank Stefano Pedri and Maurizio Chiodi (Esaote) for technical support. The work was done at the Veterinary Teaching Hospital, Department of Veterinary Medicine, University of Sassari, Sassari, Italy. The study is a part of the principal investigator (Andrea Corda) PhD thesis, defended at the University of Sassari, on March 2016. The PhD scholarship was granted by the University of Sassari.

## CONFLICT OF INTEREST DECLARATION

Authors declare no conflict of interest.

## OFF-LABEL ANTIMICROBIAL DECLARATION

Authors declare no off-label use of antimicrobials.

## INSTITUTIONAL ANIMAL CARE AND USE COMMITTEE (IACUC) OR OTHER APPROVAL DECLARATION

The study protocol was approved by the Ethical Committee of the University of Sassari (OPBSA).

## HUMAN ETHICS APPROVAL DECLARATION

Authors declare human ethics approval was not needed for this study.

## ORCID

Andrea Corda  <https://orcid.org/0000-0002-9771-4143>

## REFERENCES

- Bone RC, Balk RA, Cerra FB, et al. Definitions for sepsis and organ failure and guidelines for the use of innovative therapies in sepsis. *Chest*. 1992;101:1644-1655.
- Rau S, Kohn B, Richter C, et al. Plasma interleukin-6 response is predictive for severity and mortality in canine systemic inflammatory response syndrome and sepsis. *Vet Clin Pathol*. 2007;36:253-260.
- Mrljak V, Kučer N, Kuleš J, et al. Serum concentrations of eicosanoids and lipids in dogs naturally infected with *Babesia canis*. *Vet Parasitol*. 2014;201:24-30.
- Kalli I, Leontides LS, Mylonakis ME, et al. Factors affecting the occurrence, duration of hospitalization and final outcome in canine parvovirus infection. *Res Vet Sci*. 2010;89:174-178.
- DeClue AE, Sharp CR, Harmon M. Plasma inflammatory mediator concentrations at ICU admission in dogs with naturally developing sepsis. *J Vet Intern Med*. 2012;26:624-630.
- Torrente C, Manzanilla EG, Bosch L, et al. Plasma iron, C-reactive protein, albumin, and plasma fibrinogen concentrations in dogs with systemic inflammatory response syndrome. *J Vet Emerg Crit Care*. 2015; 25:611-619.
- Osterbur K, Whitehead Z, Sharp CR, DeClue AE. Plasma nitrate/nitrite concentrations in dogs with naturally developing sepsis and non-infectious forms of the systemic inflammatory response syndrome. *Vet Rec*. 2011;19:554-558.
- Giunti M, Troia R, Battilani M, et al. Retrospective evaluation of circulating thyroid hormones in critically ill dogs with systemic inflammatory response syndrome. *J Vet Sci*. 2017;18:471-477.
- Bauer N, Moritz A. Coagulation response in dogs with and without systemic inflammatory response syndrome - preliminary results. *Res Vet Sci*. 2013;94:122-131.
- Schaefer H, Kohn B, Schweigert FJ, Raila J. Quantitative and qualitative urine protein excretion in dogs with severe inflammatory response syndrome. *J Vet Intern Med*. 2011;25:1292-1297.
- de Laforcade AM, Freeman LM, Shaw SP, et al. Hemostatic changes in dogs with naturally occurring sepsis. *J Vet Intern Med*. 2003;17:674-679.
- Dircks BH, Mischke R, Schubert H. Platelet-neutrophil aggregate formation in blood samples from dogs with systemic inflammatory disorders. *Am J Vet Res*. 2012;73:939-945.
- O'Brien M. The reciprocal relationship between inflammation and coagulation. *Top Companion Anim Med*. 2012;27:46-52.
- Okano S, Yoshida M, Fukushima U, Higuchi S, Takase K, Hagio M. Usefulness of systemic inflammatory response syndrome criteria as an index for prognosis judgement. *Vet Rec*. 2002;150:245-246.
- Dalla K, Hallman C, Bech-Hanssen O, et al. Strain echocardiography identifies impaired longitudinal systolic function in patients with septic shock and preserved ejection fraction. *Cardiovasc Ultrasound*. 2015;13:1-10.
- Kumar A, Bunnell E, Lynn M, et al. Experimental human endotoxemia is associated with depression of load-independent contractility indices: prevention by the lipid analogue E5531. *Chest*. 2004;126:860-867.
- Parrillo JE, Burch C, Shelhamer JH, Parker MM, Natanson C, Schuette W. A circulating myocardial depressant substance in humans with septic shock. Septic shock patients with a reduced ejection fraction have a circulating factor that depresses in vitro myocardial cell performance. *J Clin Invest*. 1985;76:1539-1553.
- Stein B, Frank P, Schmitz W, Scholz H, Thoenes M. Endotoxin and cytokines induce direct cardiodepressive effects in mammalian cardiomyocytes via induction of nitric oxide synthase. *J Mol Cell Cardiol*. 1996;28:1631-1639.
- Pathan N, Hemingway CA, Alizadeh AA, et al. Role of interleukin 6 in myocardial dysfunction of meningococcal septic shock. *Lancet*. 2004; 363:203-209.
- Butler AL, Campbell VL, Wagner AE, Sedacca CD, Hackett TB. Lithium dilution cardiac output and oxygen delivery in conscious dogs with systemic inflammatory response syndrome. *J Vet Emerg Crit Care*. 2008;18: 246-257.
- Gommeren K, Desmas I, Garcia A, et al. Cardiac ultrasound in canine emergencies with a systemic inflammatory response syndrome (2012), 2012 ECVIM Congress, Oral Research Communications. *J Vet Intern Med*. 2012;26:1517.
- Nelson OL, Thompson PA. Cardiovascular dysfunction in dogs associated with critical illnesses. *J Am Anim Hosp Assoc*. 2006;42:344-349.
- Kocaturk M, Martinez S, Eralp O, Tvarijonaviciute A, Ceron J, Yilmaz Z. Tei index (myocardial performance index) and cardiac biomarkers in dogs with parvoviral enteritis. *Res Vet Sci*. 2012;92:24-29.
- Chetboul V, Serres F, Gouni V, Tissier R, Pouchelon JL. Noninvasive assessment of systolic left ventricular torsion by 2-dimensional speckle tracking imaging in the awake dog: repetibility, reproducibility, and comparison with tissue doppler imaging variables. *J Vet Intern Med*. 2008;22:342-350.
- Chetboul V, Serres F, Gouni V, Tissier R, Pouchelon JL. Radial strain and strain rate by two-dimensional speckle tracking echocardiography and the tissue velocity based technique in the dog. *J Vet Cardiol*. 2007;9:69-81.
- Wess G, Keller LJM, Klausnitzer M, Killich M, Hartmann K. Comparison of longitudinal myocardial tissue velocity, strain, and strain rate measured by two-dimensional speckle tracking and by color tissue Doppler imaging in healthy dogs. *J Vet Cardiol*. 2011;13:31-43.
- Dickson D, Shave R, Rishniw M, Patteson M. Echocardiographic assessments of longitudinal left ventricular function in healthy English Springer Spaniels. *J Vet Cardiol*. 2017;19:339-350.
- Carnabuci C, Hanås S, Ljungvall I, et al. Assessment of cardiac function using global and regional left ventricular endomyocardial and epimyocardial peak systolic strain and strain rate in healthy Labrador Retriever dogs. *Res Vet Sci*. 2013;95:241-248.



29. Spalla I, Locatelli C, Zanaboni AM, Brambilla P, Bussadori C. Speckle-tracking echocardiography in dogs with patent ductus arteriosus: effect of percutaneous closure on cardiac mechanics. *J Vet Intern Med.* 2016;30:714-721.
30. Pedro B, Stephenson H, Linney C, Cripps P, Dukes-McEwan J. Assessment of left ventricular function in healthy Great Danes and in Great Danes with dilated cardiomyopathy using speckle tracking echocardiography. *J Vet Cardiol.* 2017;19:363-375.
31. Suzuki R, Matsumoto H, Teshima T, Koyama H. Clinical assessment of systolic myocardial deformations in dogs with chronic mitral valve insufficiency using two-dimensional speckle-tracking echocardiography. *J Vet Cardiol.* 2013;15:41-49.
32. Amundsen BH, Helle-Valle T, Edvardsen T, et al. Noninvasive myocardial strain measurement by speckle tracking echocardiography: validation against sonomicrometry and tagged magnetic resonance imaging. *J Am Coll Cardiol.* 2006;47:789-793.
33. Bodey AR, Michell AR. Epidemiological study of blood pressure in domestic dogs. *J Small Anim Pract.* 1996;37:116-125.
34. Wong VM, Kidney BA, Snead ECR, Myers SL, Jackson ML. Serum C-reactive protein concentrations in healthy Miniature Schnauzer dogs. *Vet Clin Pathol.* 2011;40:380-383.
35. Lang RM, Badano LP, Mor-Avi V, et al. Recommendations for cardiac chamber quantification by echocardiography in adults: an update from the American Society of Echocardiography and the European Association of Cardiovascular Imaging. *Eur Heart J Cardiovasc Imaging.* 2015;16:233-271.
36. Cornell CC, Kittleson MD, Della Torre P, et al. Allometric scaling of M-mode cardiac measurements in normal adult dogs. *J Vet Intern Med.* 2004;18:311-321.
37. Teichholz LE, Kreulen T, Herman MV, Gorlin R. Problems in echocardiographic volume determinations: echocardiographic-angiographic correlations in the presence of absence of asynergy. *Am J Cardiol.* 1976;37:7-11.
38. Wess G, Mäurer J, Simak J, Hartmann K. Use of Simpson's method of disc to detect early echocardiographic changes in Doberman Pinschers with dilated cardiomyopathy. *J Vet Intern Med.* 2010;24(5):1069-1076.
39. Price GS, Frazier DL. Use of body surface area to calculate chemotherapeutic drug dose in dogs: I. Potential problems with current BSA formulae. *J Vet Intern Med.* 1998;12:267-271.
40. Voigt J-U, Pedrizzetti G, Lysyansky P, et al. Definitions for a common standard for 2D speckle tracking echocardiography: consensus document of the EACVI/ASE/Industry Task Force to standardize deformation imaging. *J Am Soc Echocardiogr.* 2015;28:183-193.
41. Di Bella G, Pedri S, Schreckenber M, et al. Three and four dimensional quantification of left ventricular volumes and ejection fraction on the basis of feature strain echocardiography. (2011). 72 Congresso Nazionale della Società Italiana di Cardiologia. *G Ital Cardiol.* 2011;e106:12.
42. Dragulescu A, Grosse-Wortmann L, Fackoury C, Mertens L. Echocardiographic assessment of right ventricular volumes: a comparison of different techniques in children after surgical repair of tetralogy of Fallot. *Eur Heart J Cardiovasc Imaging.* 2012;13:596-604.
43. Dukes-McEwan J, Borgarelli M, Tidholm A, Vollmar AC, Häggström J, ESVC Taskforce for Canine Dilated Cardiomyopathy. Proposed guidelines for the diagnosis of canine idiopathic dilated cardiomyopathy. *J Vet Cardiol.* 2003;5:7-19.
44. Borgarelli M, Santilli RA, Chiavegato D, et al. Prognostic indicators for dogs with dilated cardiomyopathy. *J Vet Intern Med.* 2006;20:104-110.
45. Muzzi RAL, de Araújo RB, Muzzi LAL, Pena JLB, Silva EF. Regurgitant jet area by Doppler color flow mapping: quantitative assessment of mitral regurgitation severity in dogs. *J Vet Cardiol.* 2003;5:33-38.
46. Kellihan HB, Stepien RL. Pulmonary hypertension in dogs: diagnosis and therapy. *Vet Clin North Am Small Anim Pract.* 2010;40:623-641.
47. Bland M. Clinical measurement. *An Introduction to Medical Statistics.* 3rd ed. Oxford, UK: Oxford University Press; 2000:268-293.
48. Schwarzwald CC, Schober KE, Berli ASJ, Bonagura JD. Left ventricular radial and circumferential wall motion analysis in horses using strain, strain rate, and displacement by 2D speckle tracking. *J Vet Intern Med.* 2009;23:890-900.
49. Streeter DD, Spotnirz HM, Patel DP, et al. Fiber orientation in the canine left ventricle during diastole and systole. *Circ Res.* 1969;24:339-347.
50. Antonucci E, Fiaccadori E, Donadello K, Taccone FS, Franchi F, Scolletta S. Myocardial depression in sepsis: from pathogenesis to clinical manifestations and treatment. *J Crit Care.* 2014;29:500-511.
51. Moore CC, McVeigh ER, Zerhouni EA. Noninvasive measurement of three-dimensional myocardial deformation with tagged magnetic resonance imaging during graded local ischemia. *J Cardiovasc Magn Reson.* 1999;1:207-222.
52. Reimer KA, Jennings RB. The "wavefront phenomenon" of myocardial ischemic cell death. II. Transmural progression of necrosis within the framework of ischemic bed size (myocardium at risk) and collateral flow. *Lab Invest.* 1979;40:633-644.
53. Weiss HR, Neubauer JA, Lipp JA, Sinha AK. Quantitative determination of regional oxygen consumption in the dog heart. *Circ Res.* 1978;42:394-401.
54. Kuwada Y, Takenaka K. Transmural heterogeneity of the left ventricular wall: subendocardial layer and subepicardial layer. *J Cardiol.* 2000;35:205-218.
55. Boon JA. Evaluation of size, function, and hemodynamics. *Veterinary Echocardiography.* 2nd ed. West Sussex, UK: Wiley-Blackwell; 2011:153-255.
56. Fine DM, Durham HE, Rossi NF, et al. Echocardiographic assessment of hemodynamic changes produced by two methods of inducing fluid deficit in dogs. *J Vet Intern Med.* 2010;24:348-353.
57. Burns AT, La Gerche A, D'hooge J, et al. Left ventricular strain and strain rate: characterization of the effect of load in human subjects. *Eur J Echocardiogr.* 2010;11:283-289.
58. Hamabe L, Kim S, Yoshiyuki R, et al. Echocardiographic evaluation of myocardial changes observed after closure of patent ductus arteriosus in dogs. *J Vet Intern Med.* 2015;29:126-131.
59. Owan TE, Hodge DO, Herges RM, Jacobsen SJ, Roger VL, Redfield MM. Trends in prevalence and outcome of heart failure with preserved ejection fraction. *N Engl J Med.* 2006;355:251-259.
60. Borlaug BA, Paulus WJ. Heart failure with preserved ejection fraction: pathophysiology, diagnosis, and treatment. *Eur Heart J.* 2011;32:670-679.
61. Li C, Li T, Zhang J, et al. Performance of echocardiographic parameters in sequential monitoring of left ventricular function in an animal model of acute heart failure. *Echocardiography.* 2010;27:1274-1281.
62. Serres F, Chetboul V, Tissier R, et al. Comparison of 3 ultrasound methods for quantifying left ventricular systolic function: correlation with disease severity and prognostic value in dogs with mitral valve disease. *J Vet Intern Med.* 2008;22:566-577.
63. Jacobs G, Mahjoob K. Influence of alterations in heart rate on echocardiographic measurements in the dog. *Am J Vet Res.* 1988;49:548-552.
64. Yamamoto K, Masuyama T, Tanouchi J, et al. Effects of heart rate on left ventricular filling dynamics: assessment from simultaneous recordings of pulsed doppler transmitral flow velocity pattern and haemodynamic variables. *Cardiovasc Res.* 1993;27:935-941.
65. Suzuki R, Matsumoto H, Teshima T, Koyama H. Influence of heart rate on myocardial function using two-dimensional speckle-tracking echocardiography in healthy dogs. *J Vet Cardiol.* 2013 Jun;15:139-146.
66. Weidemann F, Jamal F, Sutherland GR, et al. Myocardial function defined by strain rate and strain during alterations in inotropic states and heart rate. *Am J Physiol Heart Circ Physiol.* 2002;283:H792-H799.
67. Takano H, Fujii Y, Yugeta N, et al. Assessment of left ventricular regional function in affected and carrier dogs with duchenne muscular dystrophy using speckle tracking echocardiography. *BMC Cardiovasc Disord.* 2011;11:2-8.
68. Kenney EM, Rozanski EA, Rush JE, et al. Association between outcome and organ system dysfunction in dogs with sepsis: 114 cases (2003-2007). *J Am Vet Med Assoc.* 2010;236:83-87.
69. Parrillo JE, Parker MM, Natanson C, et al. Septic shock in humans. Advances in the understanding of pathogenesis, cardiovascular dysfunction, and therapy. *Ann Intern Med.* 1990;113:227-242.

**How to cite this article:** Corda A, Pinna Parpaglia ML, Sotgiu G, et al. Use of 2-dimensional speckle-tracking echocardiography to assess left ventricular systolic function in dogs with systemic inflammatory response syndrome. *J Vet Intern Med.* 2019;1-9. <https://doi.org/10.1111/jvim.15438>